

# Photo-Induced Orientation of Nematic Liquid Crystals in Microcapillaries

M.S. CHYCHŁOWSKI<sup>a,\*</sup>, S. ERTMAN<sup>a</sup>, M.M. TEFELSKA<sup>a</sup>, T.R. WOLIŃSKI<sup>a</sup>,  
E. NOWINOWSKI-KRUSZELNICKI<sup>b</sup> AND O. YAROSHCHUK<sup>c</sup>

<sup>a</sup>Faculty of Physics, Warsaw University of Technology, Koszykowa 75, 00-662 Warsaw, Poland

<sup>b</sup>Institute of Physics, Military University of Technology, Warsaw, Poland

<sup>c</sup>Institute of Physics of National Academy of Sciences of Ukraine, Kiev, Ukraine

Axial and transversal orientational configurations of a nematic liquid crystal 6CHBT are realized inside glassy cylindrical capillaries by using photoalignment technique. It is demonstrated that this principle can be effectively used to enforce liquid crystal alignment in the desirable direction. It can be applied to control liquid crystal alignment in the photonic crystal fibers showing great potential for the modern telecommunication technologies.

PACS numbers: 42.81.Cn, 42.79.Dj, 42.81.Pa, 42.79.Kr

## 1. Introduction

In the last years, photonic crystal fibers (PCFs) have become the subject of growing interest and intensive theoretical and experimental investigations [1–3]. Beside the conventional structures with a large number of air holes located in the silica cladding, particular attention is recently focused on the PCFs infiltrated with different materials, including nematic liquid crystals (NLCs) [4–8]. This combination enables a new way of light propagation control due to the presence of the NLC that can be easily influenced by an external factor. Photonic liquid crystal fibers (PLCFs) can be sensors of different external parameters such as temperature, pressure, electric or magnetic fields [5, 6]. Light guiding mechanism inside the PLCF can be reversibly interchanged between the modified total internal reflection (mTIR) and photonic band gap (PBG) effect [7, 8]. Except changing the light propagation mechanism in the PCF, we can change the parameters of the light propagating within a single mechanism. In case of the PBG mechanism we can tune such properties of the propagating beam as band gap wavelengths, their width and/or attenuation, whereas in case of the mTIR mechanism the width, attenuation, position of the average wavelength and polarization properties of the propagating spectrum can be modified.

Quality and stability of LC alignment as well as alignment control inside the PCF is crucial for performance of PLCF-based devices, i.e. fiber-optic sensors or optical controllers. The uniform liquid crystal (LC) alignment is commonly achieved by the directional treatment of boundary substrates limiting LC layers. These treatment methods are associated with mechanical interaction (rubbing, molding, etc.), processing with particle beams (beams of ions, radicals, atoms and plasmas) and light

beams (photoalignment) [9–11]. The majority of these methods are closely related to specific nature of the LC cells that are flat and easily accessible to cell surface. This feature makes it possible to use different techniques for the alignment treatment of these easy-access surfaces. In a result of these treatments three basic types of LC alignment can be obtained; homeotropic (perpendicular to the aligning surface), planar (parallel to the surface) and tilted (at some angle to the surface). The type of alignment depends mainly on the anchoring conditions, depending on the structure of LC and aligning material, as well as on treatment conditions.

There is, however, no such an easy-access for an inner side of a capillary with a diameter of few micrometers. For this reason any mechanically-induced alignment techniques cannot be applied. The particle beams fluxes are also extremely difficult to implement. The most promising method for this case is a photoalignment [11, 12], since the light is capable to penetrate in cavities through the glassy body of the PCF. The aim of this study is to test capability of the photoalignment technique for the LC alignment in PLCFs.

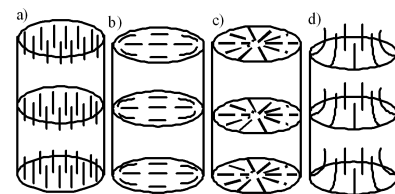


Fig. 1. Possible orientational configurations of nematic liquid crystal in a cylindric capillary with (a) planar (homogeneous, axial), (b) planar (transverse), (c) radial, (d) axial (splay) alignment.

In contrast to conventional flat capillary cells, in the cylindrical holes LC can be strongly elastically deformed.

\* corresponding author; e-mail: [opto@if.pw.edu.pl](mailto:opto@if.pw.edu.pl)

Because of this the realized orientational configuration of LC is determined by a balance of anchoring and elastic forces. This may result in a variety of orientational configurations, some of which are presented in Fig. 1. The first two structures with the planar anchoring will be realized in the present study.

## 2. Samples and alignment testing methods

A typical cladding of PCF consists of a set of cylindrical cavities with diameter about  $5\ \mu\text{m}$  [1]. To model these cavities we used cylindrical capillaries of  $8\text{--}25\ \mu\text{m}$  in diameter. The capillary walls were covered by thin layers of polyvinylcinnamate (PVCN), photoaligning polymer providing planar anchoring with the alignment direction perpendicular to polarization axis of actinic light [10–16]. For this purpose, PVCN was dissolved in chlorobenzene. First, the capillaries were filled with the PVCN solution using the high pressure enforced filling. Then, the excess of dissolved polymer was removed by the same high pressure procedure. Finally, we evaporated solvent from the prepared PVCN layer by heating up the sample above  $100\ ^\circ\text{C}$  for few minutes.

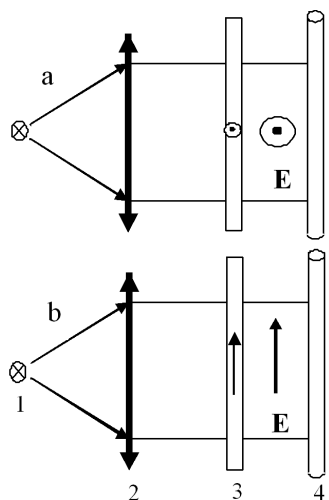


Fig. 2. Illumination schemes for planar (axial) (a) and planar (transverse) (b) alignment. 1 — UV lamp, 2 — collecting quartz lens, 3 — UV polarizer, 4 — sample.

To set alignment direction, the capillaries with the aligning layers on the inner walls were exposed to polarized light from the high pressure mercury lamp. Two different exposure geometries were used, with the UV light polarized perpendicular (Fig. 2a) and parallel (Fig. 2b) to the fiber axis. The exposure time of the sample was about 15 min.

The capillary with the photoaligning coating was infiltrated with NLC 4-trans-4'-n-hexyl-cyclohexyl-isothiocyanatobenzene (6CHBT) using the above mentioned high pressure filling. To reduce the flow-induced alignment effect, LC was heated to an isotropic state. After completion of filling and heating, the sample was cooled down to the room temperature.

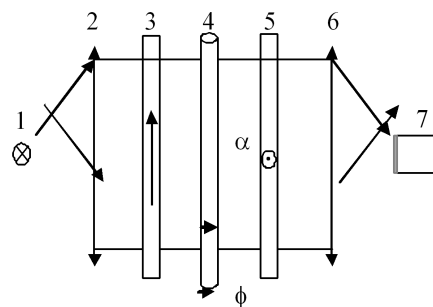


Fig. 3. Optical scheme of polarizing microscope with the sample positions during alignment inspection. 1 — light source, 2 — condenser, 3 — polarizer, 4 — samples, 5 — analyzer, 6 — objective, 7 — camera.

LC alignment in the capillaries was studied by observation of the samples in a polarizing optical microscope. The optical scheme of this experiment is presented in Fig. 3. One can see that the capillary sample was rotated around the optical axis of the system and around the long capillary axis. These rotations will be characterized by the angles  $\alpha$  and  $\phi$ , respectively. The angle  $\alpha$  is set 0 at capillary orientation parallel to the polarizer axis. In turn, the condition  $\phi = 0$  is assigned to the capillary position corresponding to minimization of light transmittance, if this minimization is observable. The interferometric polarizing microscopy was used as an additional tool for the alignment evaluation; it used the birefringence of LC inside the capillary as the measure of the alignment quality.

## 3. LC alignment

### 3.1. Planar (axial) alignment

The planar configuration (Fig. 1a) was realized by irradiating a capillary internally coated by a photoaligning film with a UV light polarized perpendicular to the fiber axis (Fig. 2a). Figure 4 shows pictures of this sample for different values of angles  $\alpha$  and  $\phi$ . The sample transmittance was minimized at  $\alpha = 0^\circ$  and  $\alpha = 90^\circ$  and maximized at  $\alpha = 45^\circ$  irrespective of value of angle  $\phi$ . This means that LC molecules are preferably aligned along the capillary axis. Rotation of the sample positioned at  $\alpha = 45^\circ$  around its long axis did not bring visible change of the transmittance (Fig. 4d). This implies that the induced LC configuration has an axial symmetry as depicted in Fig. 1a.

It should be noticed that a similar structure was observed in the capillaries without alignment layers. The quality of LC alignment in these capillaries was, however, much lower as in the capillary with photoaligning layer demonstrated in Fig. 4. Photoaligned layer is not affected by the flow-induced alignment due to heating LC to isotropic state after the filling procedure.

The alignment quality in this configuration was additionally checked by estimation of LC birefringence in the

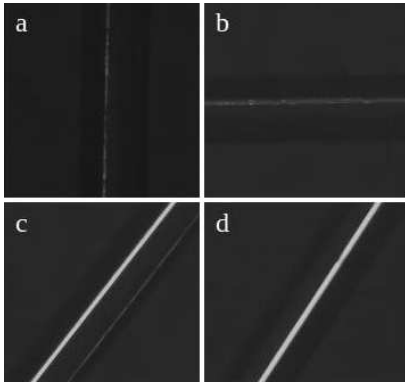


Fig. 4. The sample with planar LC configuration under the polarizing microscope. (a)  $\alpha = 0^\circ$ , (b)  $\alpha = 90^\circ$ , (c)  $\alpha = 45^\circ$ ,  $\phi = 90^\circ$ , (d)  $\alpha = 45^\circ$ ,  $\phi = 0^\circ$ ,  $\times 100$  magnification.

capillary by the interferometric polarizing microscope. The image of the samples with a diameter of  $25 \mu\text{m}$  viewed in this microscope is shown in Fig. 5. The pronounced shift of interference patterns in the sample is caused by essential phase retardation in the LC volume. The birefringence  $\Delta n$  of LC can be evaluated from Fig. 5 by using the formula

$$\Delta n = \lambda \frac{d}{h D}, \quad (1)$$

where  $D$  is a diameter of a capillary tube ( $25 \mu\text{m}$ ) filled with the LC,  $\lambda$  is an average wavelength ( $550 \text{ nm}$ ),  $h$  is a distance between two maxima and  $d$  is a shift of maximum. The ratio  $d/h$  is equal to 6.8 and corresponds to the birefringence 0.15. This value agrees with the tabulated value of  $\Delta n$  for LC 6CHBT [17–19] and confirms that the LC is in the highly ordered state.

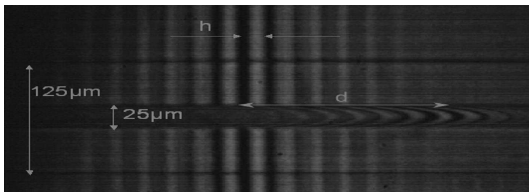


Fig. 5. Image of LC capillary ( $D = 25 \mu\text{m}$ ) with axial alignment configuration in optical interferometric microscope.

### 3.2. Transverse alignment

Transverse orientation was achieved by irradiating a thin layer of the photoactive polymer in a capillary by using a UV light polarized parallel to the fiber axis (Fig. 1b). The images of this sample in optical polarizing microscope are collected in Fig. 6. It is evident that at  $\alpha = 0^\circ$  and  $\alpha = 90^\circ$  the sample reaches minimum of transmittance irrespective of angle  $\phi$ . At the same time, at  $\alpha = 45^\circ$  the transmittance considerably depends on  $\phi$ ;

rotation of the sample around its long axis results in oscillation of optical transmittance with the period of  $90^\circ$ . Taking into account these features as well as the alignment direction of PVCN layers perpendicular to the light polarization [10–16] one can deduce that the transversal configuration presented in Fig. 1b is realized. It is formed in a result of a balance of anchoring and elastic forces and somewhat reminds the bipolar structure of LC director within the capsules with planar anchoring conditions formed in polymer dispersed liquid crystals [20–22]. It is worthwhile mentioning that during formation of the transversal configuration the flow-induced alignment counteracts with the effect of photoalignment. This means that isotropic state of LC during filling and some time after filling (to eliminate memorization of flow-induced alignment) should be thoroughly controlled.

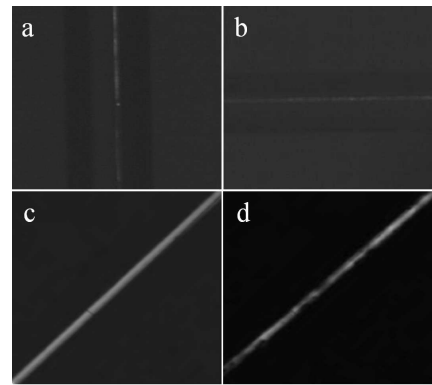


Fig. 6. The sample with transversal LC configuration under the polarizing microscope. (a)  $\alpha = 0^\circ$ , (b)  $\alpha = 90^\circ$ , (c)  $\alpha = 45^\circ$ ,  $\phi = 90^\circ$ , (d)  $\alpha = 45^\circ$ ,  $\phi = 0^\circ$ ,  $\times 100$  magnification.

Finally note that both axial and transversal alignment configurations described above were realized in fibers of all diameters from the range  $8\text{--}25 \mu\text{m}$ . This means that in this whole range the photoalignment factor strongly dominates and determines LC alignment.

## 4. Conclusions

The axial and transverse LC configurations are realized in the cylindrical capillaries. This was achieved by using photoaligning material providing planar anchoring conditions. It is demonstrated that the alignment direction is effectively controlled by the polarization direction of the light. We believe that the field of LC structures obtainable by the photoalignment technique is much broader and our further attempts will be aimed to their realization. The results obtained give possibility of an application of the same procedure to induce LC orientation in PCFs. Controlling of LC anchoring will improve repeatability of PLCFs and can increase a tuning range of the fiber birefringence.

### Acknowledgments

This work was supported by the Polish Ministry of Science and Education under the grant N517 056535 and partially by the “Master” Programme of the Polish Science Foundation. The work was partially supported by the European Union in the framework of European Social Fund through the Warsaw University of Technology Development Programme.

### References

- [1] J.C. Knight, *Nature* **424**, 847 (2003).
- [2] R. Buczynski, *Acta Phys. Pol. A* **106**, 141 (2004).
- [3] P.St.J. Russell, *J. Lightwave Technol.* **24**, 4729 (2006).
- [4] S. Ertman, T.R. Woliński, A. Czapla, K. Nowecka, E. Nowinowski-Kruszelnicki, J. Wójcik, *Proc. SPIE* **6587**, 658706 (2007).
- [5] F. Du, Y. Lu, S.-T. Wu, *Appl. Phys. Lett.* **85**, 2181 (2004).
- [6] T. Larsen, A. Bjarklev, D. Hermann, J. Broeng, *Opt. Express* **11**, 2589 (2003).
- [7] T.R. Wolinski, K. Szaniawska, S. Ertman, P. Lesiak, A.W. Domański, in: *Proc. Symp. on Photonics Technologies for 7th Framework Program*, Ed. A. Popiolek-Masajada, Oficyna Wydawnicza Politechniki Wrocławskiej, Wrocław 2006, p. 95.
- [8] J. Sun, C.C. Chan, *J. Opt. Soc. Am. B* **24**, 2640 (2007).
- [9] K. Takato, M. Hasegawa, M. Koden, N. Itoh, R. Hasegawa, M. Sakamoto, *Alignment Technologies and Applications of Liquid Crystal Devices*, Taylor and Francis, London 2005.
- [10] V. Chigrinov, *Photoalignment of Liquid Crystal Materials: Physics and Application*, Wiley-SID Series, UK 2008.
- [11] Hiroshi Kawamoto, *Proc. IEEE* **90**, 460 (2002).
- [12] M. O’Neill, S.M. Kelly, *J. Phys. D, Appl. Phys.* **33**, R67 (2000).
- [13] M. Schadt, K. Schmitt, V. Kozenkov, V. Chigrinov, *Jpn. J. Appl. Phys. Part 1* **31**, 2155 (1992).
- [14] A. Dyadyusha, T. Marusii, Y. Reznikov, A. Khizhnyak, V. Reshetnyak, *JETP Lett.* **56**, 17 (1992).
- [15] G.P. Bryan-Brown, I.C. Sage, *Liq. Cryst.* **20**, 825 (1996).
- [16] O. Yaroshchuk, T. Sergan, J. Kelly, I. Gerus, *Jpn. J. Appl. Phys.* **41**, 275 (2002).
- [17] J. Baran, Z. Raszewski, R. Dabrowski, J. Kedzierski, J. Rutkowska, *Mol. Cryst. Liq. Cryst.* **123**, 237 (1985).
- [18] R. Dabrowski, J. Dziaduszek, T. Szczucinski, *Mol. Cryst. Liq. Cryst.* **124**, 241 (1985).
- [19] Y.V. Izdebskaya, V.G. Shvedov, A. Desyatnikov, W. Krolikowski, M. Belic, G. Assanto, Y. Kivshar, *Opt. Express* **18**, 3258 (2010).
- [20] D. Budaszewski, A. Domanski, *Acta Phys. Pol. A* **116**, 285 (2009).
- [21] A. Domański, P. Lesiak, K. Milenko, D. Budaszewski, M. Chychłowski, S. Ertman, M. Tefalska, T.R. Woliński, K. Jędrzejewski, L. Lewandowski, W. Jasiewicz, J. Helsztyński, A. Boczkowska, *Acta Phys. Pol. A* **116**, 294 (2009).
- [22] P.S. Drzaic, *Liquid Crystal Dispersions*, Vol. 1, Series on Liquid Crystals, World Sci., Singapore 1995.